Bimodality of Sparse Autoencoder Features is Still There and Can Be Fixed

Michał Brzozowski
Samsung AI Research Center, Warsaw, Poland
m.brzozowsk3@samsung.com

Abstract

Sparse autoencoders (SAE) are a widely used method for decomposing LLM activations into a dictionary of interpretable features. We observe that this dictionary often exhibits a bimodal distribution, which can be leveraged to categorize features into two groups: those that are monosemantic and those that are artifacts of SAE training. The cluster of noninterpretable or polysemantic features undermines the purpose of sparse autoencoders and represents a waste of potential, akin to dead features. This phenomenon is prevalent across autoencoders utilizing both ReLU and alternative activation functions. We propose a novel training method to address this issue and demonstrate that this approach achieves improved results on several benchmarks from SAEBench.

1 Introduction

1.1 The Dawn of SAEs and the Forgotten Phenomenon

The superposition hypothesis [12] posits that deep learning models represent more features than they have neurons through linear directions. In [33], the authors demonstrated that the simple architecture of sparse autoencoders (SAE) can perfectly "disentangle" superposition in a synthetic dataset. In this toy model scenario, we have access which features (directions in the activation space) are ground truth. The key challenge when applying SAEs to real language data lies in measuring a quality of features when there is no ground truth. The proposed method involves the following steps:

- Train a sparse autoencoder A on a dictionary of size N.
- Train another sparse autoencoder B on a dictionary of a larger size.
- Check what features are similar between the two by measuring **maximal cosine similarity (MCS)** between feature i from A and the entire dictionary from the larger dictionary B.

The rationale is that features identified independently by two dictionaries are, in a sense, "universal." Following this procedure, for every feature i, a scalar score MCS_i is obtained, which serves as a proxy for feature quality, monosemanticity, or universality. Surprisingly, it was soon observed that these scores follow a clear bimodal distribution [10]. Moreover, the lower values cluster closely with the distribution of randomly generated vectors [16]. Subsequent manual and automatic approaches to interpretability [4] confirmed that the MCS value is positively correlated with feature monosemanticity. In [30], the authors manually inspected features by sorting them in descending order based on the MCS score and discovered that the top-ranked features are monosemantic. Furthermore, [9] demonstrated that the top-150 MCS features exhibit higher interpretability scores compared to random ones.

39th Conference on Neural Information Processing Systems (NeurIPS 2025) Workshop: Mechanistic Interpretability.

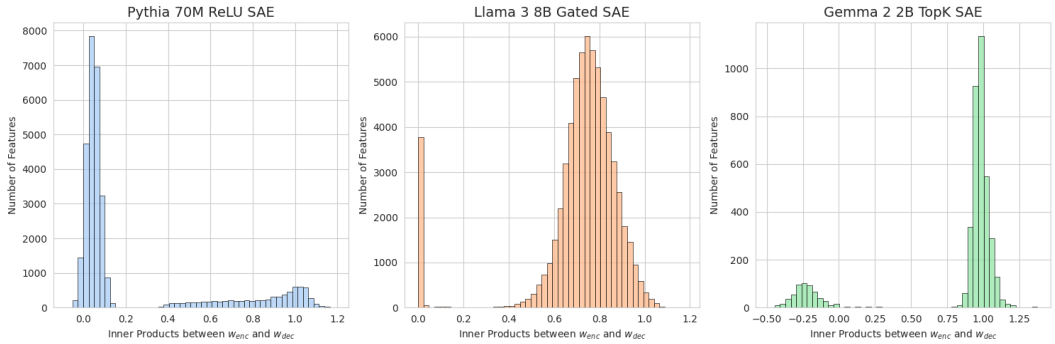

Figure 1: We can observe the bimodality of SAE features across different models and SAE architectures.

1.2 A Simpler Feature Quality Proxy

The observation that MCS scores can be used to assess the quality of SAE features and distinguish between "true" directions and random artifacts appears to have been overlooked. This insight is notably absent in the main culmination paper [17] and is only briefly mentioned in a footnote in the independent Anthropic work [6]. We speculate that the primary reason for its neglect is the computational cost of the described method, as calculating MCS scores necessitates training an additional larger dictionary.

In our work, we revisit this idea by:

- Proposing a simpler scalar proxy for feature quality that does not require any data or additional training: the inner product between the encoder and decoder
- Demonstrating that this score remains bimodal even in modern SAE variants, such as TopK, Gated, and JumpReLU.
- Establishing a positive correlation between the proposed score and the autointerpretability score.
- Proposing a novel training method to eliminate bimodality by design.
- Demonstrating that the proposed method outperforms standard training across multiple benchmarks, models, dictionary sizes, sparsities, and activation functions.

2 Background on Sparse Autoencoders

Let $\mathbb{R}^n$ represent the activation space of a deep learning model, such as the residual stream of a large language model (LLM). The goal of a sparse autoencoder (SAE) is to decompose the activation of a data point into a sparse linear combination of features from a dictionary of size m. It has been shown [17, 6] that such features are more interpretable than neuron basis.

The encoder and decoder parts are defined as follows:

$$\mathbf{f}(\mathbf{x}) := ReLU(W^{enc}\mathbf{x} + \mathbf{b}^{enc}),$$

$$\hat{\mathbf{x}} := W^{dec}\mathbf{f}(\mathbf{x}) + \mathbf{b}^{dec},$$

where $\mathbf{f}(\mathbf{x}) \in \mathbb{R}^m$ is the sparse latent vector and $\hat{\mathbf{x}} \in \mathbb{R}^n$ is the reconstructed output, $W^{enc} \in \mathbb{R}^{m\times n}$, $W^{dec} \in \mathbb{R}^{n\times m}$ are the encoder and decoder matrices, respectively, $\mathbf{b}^{enc} \in \mathbb{R}^m$, $\mathbf{b}^{dec} \in \mathbb{R}^n$ are the encoder and decoder biases, respectively.

The loss is a weighted sum of the reconstruction L^2 loss and the L^1 penalty to enforce sparsity. That is

$$\mathcal{L} = \mathcal{L}_R + \lambda\mathcal{L}_P,$$

where

$$\mathcal{L}_R = \|\hat{\mathbf{x}} - \mathbf{x}\|^2$$

and

$$\mathcal{L}_P = \|\mathbf{f}(\mathbf{x})\|_1 .$$

The scalar λ is a tunable hyperparameter that controls the sparsity of the autoencoder. An important property of these equations is their homogeneity: multiplying the encoder and dividing the decoder by any scalar results in the same reconstruction. Without additional constraints, training could *cheat* by making the sparsity loss $\mathcal{L}_P$ arbitrary small. This seemingly straightforward issue requires nontrivial solutions. Two methods have been proposed by researchers:

Normalization of the columns of the decoder matrix W^{dec} [6, 17]. This approach requires careful synchronization with gradient updates. In [6, 15], authors project away gradient information parallel to the decoder vectors to account for interactions between the Adam optimizer and normalization. In the code [32], authors implement a constrained version of the Adam optimizer instead.

Reformulation was used instead in [8]. More precisely, they change the L^1 norm to the weighted norm with the weights being equal to the L^2 norms of the decoder columns:

$$\mathcal{L}_P = \sum_i \mathbf{f}_i(\mathbf{x})||W^{dec}_{\cdot,i}||_2.$$

This reformulation solves the homogeneity problem. Indeed, the trick with multiplication and division by the same scalar does not affect the proposed $\mathcal{L}_P$. In line with this best practice, we also use the reformulation method and do not normalize the decoder columns.

We have detailed this homogeneity problem because a deep understanding of underlying symmetries is crucial for identifying better inductive biases. Indeed, in the main section of our work (5), we will apply a novel reformulation method to eliminate sparse autoencoder feature bimodality.

In this paper, we primarily analyze and improve standard ReLU sparse autoencoders. However, we will also mention alternative architectures, such as TopK [15], Gated [28], and JumpReLU [29], which employ different activation functions and training procedures.

3 Measuring alignment between encoder and decoder

3.1 Alignment Score — Heuristic Motivation

According to the **linear representation hypothesis** (and the related **superposition hypothesis**), deep learning models represent concepts as directions in the activation space. SAEs learn these directions in an unsupervised manner. Indeed, each feature $i \in \{1, \dots m\}$ corresponds to the row vector $W^{enc}_{i,\cdot}$ and the column vector $W^{dec}_{\cdot,i}$. It is not clear which of them is the *true* feature vector. In practice, the encoder vector is used for the concept detection and the decoder vector is used for the model steering (see details in [35]). Observe that intuitively these two vectors (the encoder and decoder ones) should be similar. Indeed, in [17], the authors use this rationale to tie the encoder and decoder weights, that is: (see the footnote 2 there) $W^{enc} = (W^{dec})^T$. In the tied weights scenario, both vectors coincide (assuming normalization). However, this is not a common practice, and most modern SAEs do not adopt this procedure.

Based on this intuition, we propose the following measure as a proxy for feature quality:

$$a_i = W^{enc}_{i,\cdot} \cdot W^{dec}_{\cdot,i}, \tag{1}$$

where $i \in \{1, \dots m\}$ and $\cdot$ is the inner product in $\mathbb{R}^n$. Equivalently, these is i-th diagonal element of the matrix product $W^{enc}W^{dec}$. We suspect that values of a_i which are negative or close to 0 correspond to not interpretable features which are the artifact of SAE training. We refer to these scalars as **alignment scores**.

While the motivation for this section is based on heuristics, we also provide more precise arguments for introducing this score, grounded in an analysis of toy models, in the next subsection. One of the main reasons for using the inner product formulation is the homogeneity property described in the previous subsection. Note that the alignment score (Equation 1) remains invariant with respect to multiplication of the encoder and division of the decoder by the same scalar. We emphasize that

preserving this structural algebraic property is crucial in constructing the alignment score. This motivates the choice of the inner product over, perhaps more intuitive, cosine similarity, which exhibits stronger scale invariance with respect to both variables.

3.2 Alignment Score Should be Close to 1 - Toy Model Argument

In this subsection we will show that the alignment score is not just an ad-hoc formula and show that it should be cluster close to 1. This will be confirmed empirically in the experiments.

Let us consider one of the simplest toy model: the activation space is two dimensional, that is $n = 2$ and there is only one feature in a sparse autoencoder $m = 1$. Moreover, we ignore biases and use the training set of just a one single point $\mathbf{x} \in \mathbb{R}^2$. We also ignore the sparsity penalty, so the setting is:

$$f(\mathbf{x}) = ReLU(w^{enc} \cdot \mathbf{x}),$$
$$\hat{\mathbf{x}} = f(\mathbf{x})w^{dec},$$

where w^{enc} and w^{dec} are vectors and $\cdot$ denotes an inner product in $\mathbb{R}^2$. The latent $f(\mathbf{x})$ is just a scalar because we set $m = 1$.

Naturally, this is a very artificial setting and the autoencoder can just learn the identity. However, as we will see, the ReLU nonlinearity makes the training dynamics not that trivial. Now let us check, when this toy model can perfectly reconstruct the input, that is when $\hat{\mathbf{x}} = \mathbf{x}$. We have:

$$\mathbf{x} = ReLU(w^{enc} \cdot \mathbf{x})w^{dec}$$

Observe that $\mathbf{x}$ and w^{dec} must be parallel, so $\mathbf{x} = \alpha w^{dec}$ for some scalar constant α. Hence we obtain

$$\alpha w^{dec} = ReLU(\alpha w^{enc} \cdot w^{dec})w^{dec}.$$

This leads to our desired equation:

$$1 = w^{enc} \cdot w^{dec}.$$

In fact, this single training point example was the first "experiment" done in this research project and the connection with the MCS and the bimodality phenomenon were discovered later.

The presented toy experiment is very crude and simplified, but as we will see, it scales effectively to real sparse autoencoders. It mirrors the illustrative example from [2], which the authors used to explain the feature suppression/shrinkage effect.

4 Preliminary Experiments

4.1 Experiment 1: Alignment Scores Are Bimodal

In the first experiment, we calculated the histograms of the alignment scores. The results are presented in Figure 1. Across different models and SAE architectures, we observed that the score distribution is consistently bimodal. We suspect that this bimodality is similar to the phenomenon discovered by Huben [16]. Additionally, a footnote in the Anthropic work [6] speculates that this same bimodality corresponds to feature frequency. It is important to emphasize that, unlike MCS, the alignment score is calculated without training an additional larger SAE. Furthermore, unlike feature frequency, it is derived directly from the weights without requiring additional language corpus data.

4.2 Experiment 2: Alignment Scores Are Highly Correlated with MCS

In the next experiment, we compared the MCS scores with the alignment scores for an autoencoder trained on MLP activations from the second layer of Pythia [3]. We utilized the SAE from [30], where SAEs of different sizes are available. This approach avoided the need to train a larger autoencoder from scratch, which would otherwise be required to calculate MCS. The resulting scatter plot is shown in Figure 2. The Pearson correlation coefficient is high, with a value of 0.65. Additionally, as observed, low alignment scores correspond to weaker features that were not discovered by a larger interpreter model. The cluster of the best features concentrates at an alignment value of 1.0 as predicted by the toy model argument from 3.2.

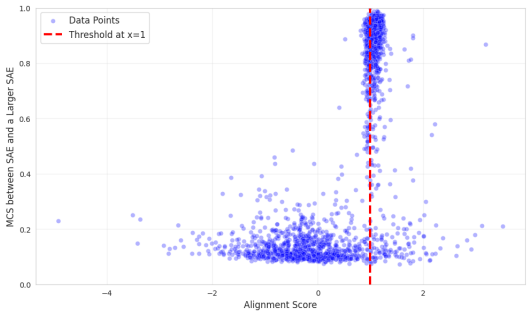

Figure 2: The scatter plot of MCS vs the alignment score. The Pearson correlation is high and equal to 0.65. The red vertical line denotes the alignment score value equal to 1.

4.3 Experiment 3: Alignment Scores can be Used to Find Interpretable Features

In the previous experiment, we compared one proxy with another. Here, we directly assess whether alignment scores can be used to evaluate feature interpretability. We apply the commonly used autointerpretability protocol introduced in [4]. In this method, LLM judge first generates a natural language description of a given neuron or direction based on a sample of maximal activations. Then, the judge model uses this generated description to score each token in another sample of texts. The interpretability score is the Pearson correlation between the LLM judge scores per token and the actual activation scores. In the case of SAEs, the activation score for feature i is equal to the encoder value $\mathbf{f}_i(\mathbf{x})$. For more details on autointerpretability protocols, see [27].

The resulting scatter plot comparing the alignment scores with autointerpretability is presented in figure 3. The dead features for which we did not have enough non-zero activation to run the autointerpretability are presented as black dots.

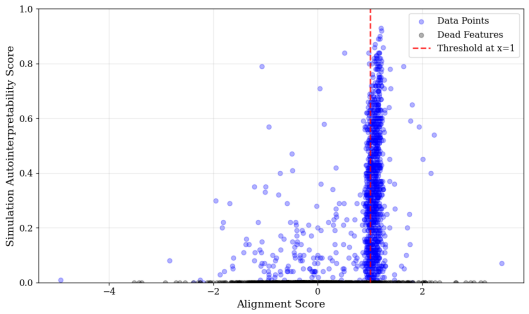

Figure 3: Autointerpretability scores vs the alignment score. The red vertical line denotes the alignment score value equal to 1. The Pearson correlation is equal to 0.32.The Pearson correlation is equal to 0.32.

5 Fixing Bimodality

From a practical standpoint, having a measure of feature quality can aid in designing more effective training algorithms for SAEs. This idea has been suggested in [10] in the context of MCS: *"Also, the bimodal nature of the MCS scores suggests that we might be able to use unorthodox training strategies where we identify the convergent features and then perhaps freeze them while aggressively perturbing the remaining vectors."* While implementing this with the demanding MCS score was challenging, the overall simplicity of the proposed alignment score makes it feasible. Additionally, feature-aligned sparse autoencoders [25] employ a similar approach, requiring the training of two sparse autoencoders in parallel and resampling. In contrast, we propose a straightforward algebraic transformation. As discussed in 2, the encoder and decoder are defined as follows:

$$\mathbf{f}(\mathbf{x}) := ReLU(W^{enc}\mathbf{x} + \mathbf{b}^{enc}),$$
$$\hat{\mathbf{x}} := W^{dec}\mathbf{f}(\mathbf{x}) + \mathbf{b}^{dec},$$

Now, the key idea is to leave $\mathbf{b}^{enc}, \mathbf{b}^{dec}$ and W^{dec} as arbitrary trainable parameters and modify W^{enc}. In the proposed training method we instead of W^{enc} use a trainable parameter matrix $A \in \mathbb{R}^{m \times n}$ and define an encoder row $W^{enc}_{i,\cdot}$ as:

$$W^{enc}_{i,\cdot} := A_{i,\cdot} + \alpha_i W^{dec}_{\cdot,i}, \tag{2}$$

where

$$\alpha_i = \frac{1 - A_{i,\cdot} \cdot W^{dec}_{\cdot,i}}{||W^{dec}_{\cdot,i}||^2}.$$

It is straightforward to check that:

$$W^{enc}_{i,\cdot} \cdot W^{dec}_{\cdot,i} = 1, \tag{3}$$

for every $i = 1, \ldots, m$.

Now, we just use the standard gradient descent training for parameters $b^{enc}, b^{dec}, W^{dec}$ and A.

In essence, we constrain the manifold of possible weights by enforcing the equation 3. Our conjecture is that this inductive bias can enhance the training of the sparse autoencoder. This approach is similar in spirit to convolutional networks. Indeed, every convolutional layer is essentially a linear layer constrained by the local receptive field [13] and weight sharing [23]. In theory, a linear layer could learn convolution during training, but incorporating this inductive bias makes the training of computer vision models more effective.

We will refer to the proposed method as **aligned training** and demonstrate that it outperforms standard ReLU autoencoders on several benchmarks across different sparsities, dictionary sizes, and underlying language models.

Moreover, because equation 3 constrains every encoder row to lie on an affine hyperplane of dimension $n - 1$, we can set the last column of A to 0 (and not train it). The resulting model can still express the same space of weights. In other words, we achieve **compression for free**; an autoencoder from aligned training has slightly fewer parameters.

5.1 Experiment 4: Aligned Training Achieves Pareto Improvement on Reconstruction Metrics

The most basic metric used to evaluate the quality of any autoencoder is its ability to reconstruct the input. For comparing sparse autoencoders, it is essential to measure reconstruction across different sparsities, as less sparse autoencoders can trivially achieve better reconstruction (and, in the limit, even learn the identity function). The sparsity is measured by L_0 "norm", which is the number of nonzero values in the encoded vector $\mathbf{f}(\mathbf{x})$.

Following [7, 22] we use two methods to check how good is the the autoencoder reconstruction: the explained variance and the recovered cross entropy loss (consult the Appendix B for precise formulas of these metrics).

We trained the ReLU autoencoders on the 50 million tokens from the Pile [14] using both the standard and the aligned methods and performed the test on OpenWebText. The results are presented in the figure 4. The aligned method outperforms standard training across two models, four sparsities and three dictionary sizes (see figures 12, 14 in the Appendix D for 16K and 65K dictionary sizes).

5.2 Experiment 5: Aligned Training as a Parameter-Free Method to Avoid Dead Features

One of the notorious issues in training sparse autoencoders is the problem of dead features, where a feature does not activate for any token [6, 15, 18]. This occurs because it is an easy way to minimize the sparsity loss. Several advanced measures have been developed to reduce the number of dead features:

- Resampling schemes with non-uniform probabilities [6].

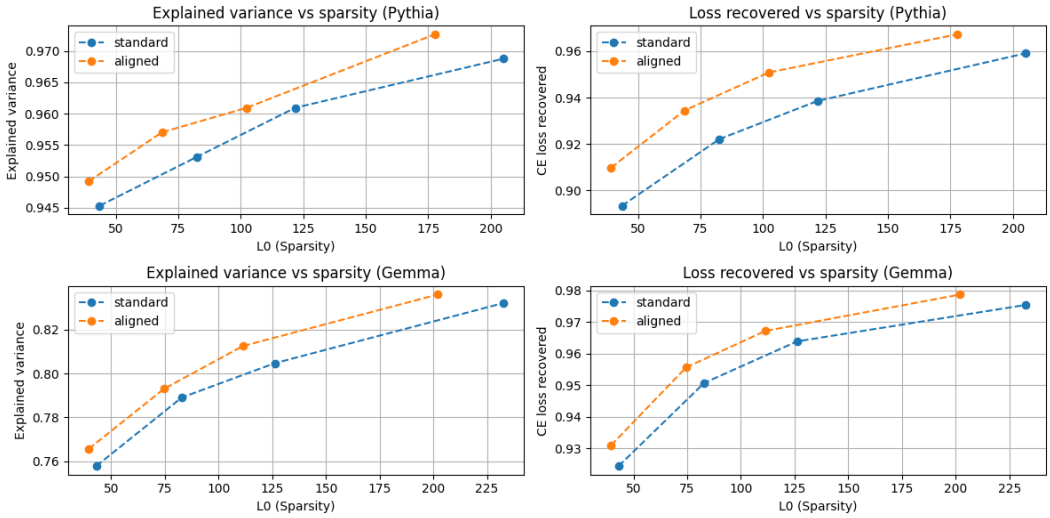

Figure 4: The proposed training methods improves the recovered cross entropy of sparse autoencoder across different sparsities. The results for the dictionary size 4096 for the 8th layer of the Pythia 160M and the 12th layer of Gemma 2 2B [34]

- Adding artificial gradients, known as *ghost grads*, which were introduced briefly by Anthropic [18] but later abandoned due to their role in causing loss spikes [1].
- Introducing an auxiliary loss term for dead features, as proposed in the TopK autoencoder paper [15].

We emphasize that all these methods require extensive hyperparameter tuning. In contrast, our proposed aligned training completely eliminates dead features: see Figure 5. The aligned training is parameter-free and does not require sampling or other non-differentiable operations that could destabilize training. As shown, the standard ReLU sparse autoencoder has approximately 20% dead neurons, while the aligned autoencoder has none. Furthermore, resampling and ghost grad methods focus on resurrecting dead features, whereas aligned training constrains the parameter space to prevent features from dying in the first place.

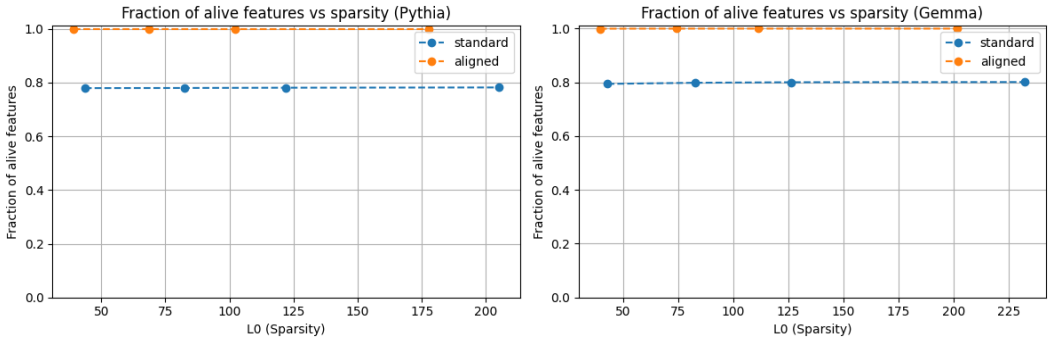

Figure 5: The proposed training method is a parameter-free approach significantly reducing the number of dead features. The results for the dictionary size 4096 for the 8th layer of the Pythia 160M and 12th layer of Gemma 2 2B.

5.3 Experiment 6: Aligned Training Outperforms Standard Autoencoder in Spurious Correlation Removal

The metrics used in the two previous experiments are still theoretical proxies for evaluating the usefulness of an autoencoder. We also tested our proposed method on a practical downstream task

and found that it achieves better results. The application of sparse autoencoders to remove spurious correlations was introduced in the SHIFT method [26] in the context of gender bias [11] and extended in [20]. We used the implementation of this metric from the SAEBench suite [22].

As shown in Figure 6, aligned training outperforms the standard method on the Pythia model. For Gemma, the two methods are comparable for smaller sparsity ranges, but our method shows a clear advantage for larger L_0 values.

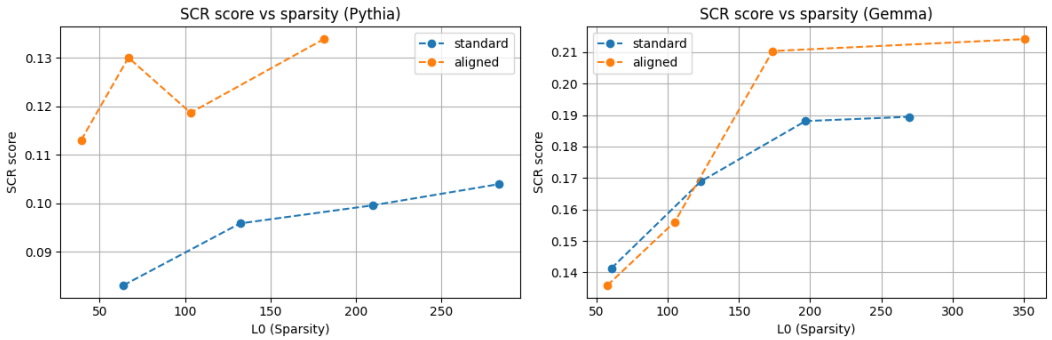

Figure 6: Results for spurious correlation removal metric from SAEBench on the dictionary size = 65K for Pythia 160M and Gemma 2 2B.

5.4 Experiment 7: Exploratory Analysis of Feature Distributions Between Standard and Aligned Training

In Figure 7, we compare the alignment scores between similar sparsity autoencoders trained using both standard and aligned methods. For the standard autoencoder, we observe bimodality in the distribution. Notably, the 800 features with alignment scores close to 0 correspond to approximately 20% of the dead features (for a dictionary size $m = 4096$). The attractor at 0, which causes features to die, is similar to the histogram observed in Figure 1 for the Gated autoencoder.

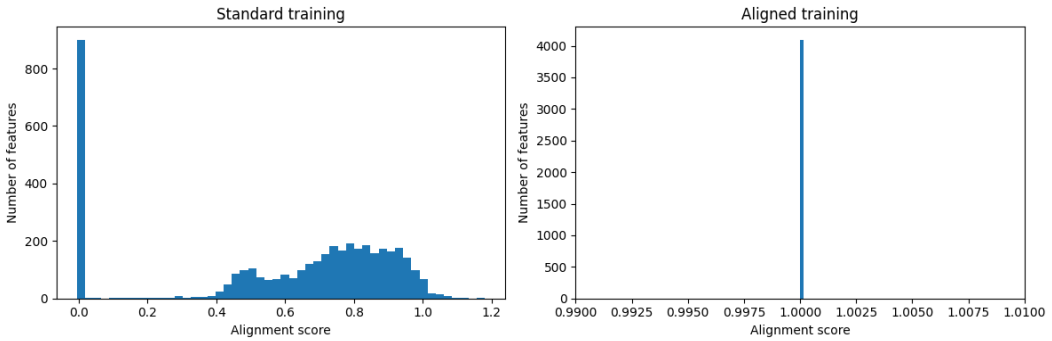

Figure 7: Histograms of alignment scores of the standard and aligned trained sparse autoencoders. The plot on the right serves as a sanity check: the proposed reformulation achieves its intended goal by forcing all alignment scores to be equal to 1, effectively preventing the creation of bimodality.

5.5 Experiment 8: Scaling Training to 500M Tokens and Comparing to State-of-the-Art

In this section, we compare aligned training to state-of-the-art ReLU sparse autoencoders provided by SAEBench. To ensure a fair comparison, we scale our training to **half a billion tokens** from The Pile [14], matching the compute used in SAEBench (recall that our formula was derived from a **1-token** toy model). As shown in Figure 8, our training surpasses both the standard SAEs trained by us and those provided by the benchmark authors. This demonstrates that the advantage is robust and not a result of cherry-picking hyperparameters. Additionally, Figure 9 shows that our training achieves a significantly lower number of dead features.

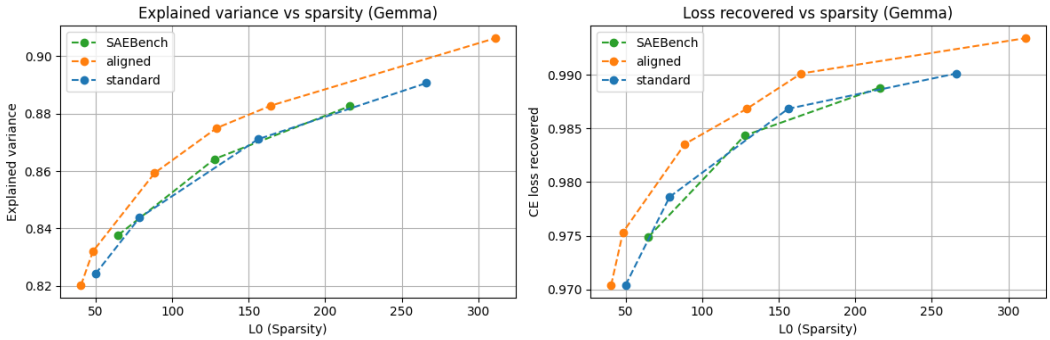

Figure 8: Reconstruction metrics comparing our method to standard (trained by us) and state-of-the-art checkpoints provided by SAEBench. Training was conducted on half a billion tokens for layer 12 of Gemma 2 2B with a dictionary size of 65K features.

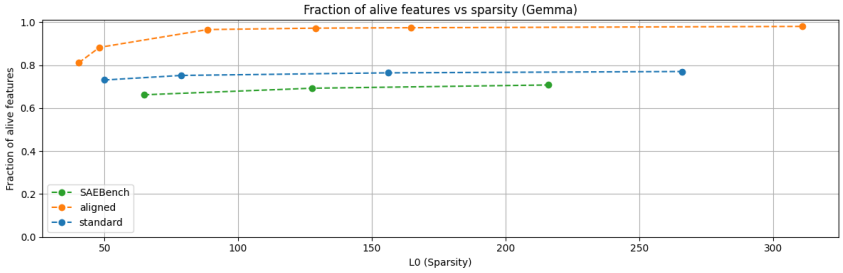

Figure 9: Fraction of alive features comparing our method to standard (trained by us) and state-of-the-art checkpoints provided by SAEBench. Training was conducted on half a billion tokens for layer 12 of Gemma 2 2B with a dictionary size of 65K features.

6 Preliminary results for TopK sparse autoencoders

In this section we provide the results for applying the aligned training method for the newer architecture of TopK sparse autoencoder [15]. In this approach, the sparsity is enforced not by the L^1 penalty, but by the TopK activation applied on top of $\mathbf{f}(\mathbf{x})$ (as we described in the section 2). Notice, that our training reformulation 5 can be directly applied also in this case. While the primary motivation and toy model argument were based on the ReLU model, it turns out that similar improvements can be achieved even with the TopK approach.

Figure 10 presents the results of training TopK autoencoders on 50 million tokens from The Pile using both the standard TopK and the aligned method. The proposed training method outperforms the baseline in the low-sparsity regime, while for higher sparsities, there is no significant difference between the two. Furthermore, the same pattern is observed in the number of dead neurons, as shown in Figure 11.

7 Limitations

Experiments were restricted to the ReLU setting. In this work, we focused on standard sparse autoencoders (sometimes referred to as *vanilla* [29]). As shown in the first figure, bimodality also appears for different activation functions.In future work, we plan to extend our method to newer architectures. While we conducted preliminary experiments on TopK sparse autoencoders in the previous section, further investigation is needed to explore the relationship between sparsity, reconstruction, and dead neurons.

We compared aligned training only to the standard protocol. There are several non-standard methods for training ReLU autoencoders, such as square root [24], tanh [19], and p-annealing [21]. These methods were introduced to address the issue of feature shrinkage [2]. Our work was motivated

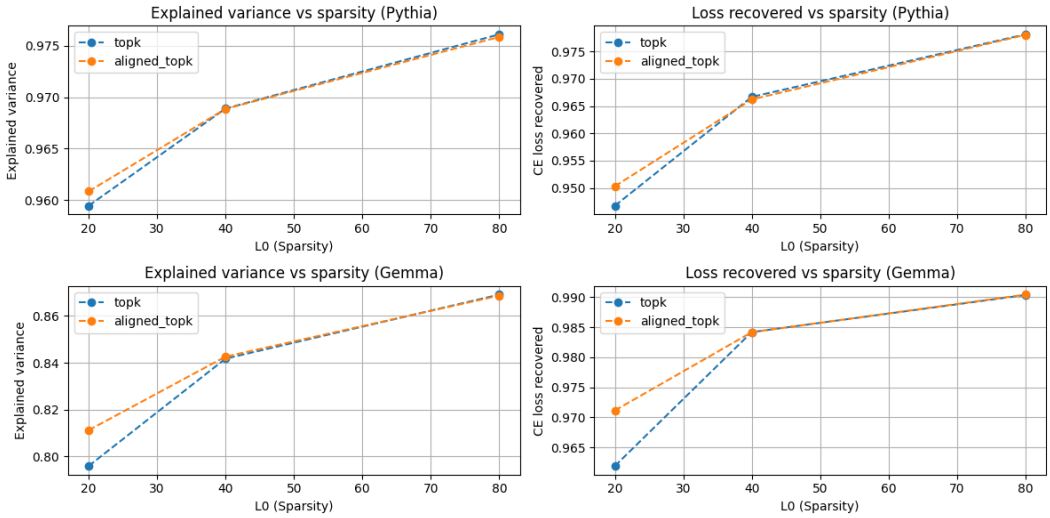

Figure 10: The proposed training methods improves the recovered cross entropy of the TopK sparse autoencoder for low sparsity. However, for larger sparsities the difference is negligible. The results for the dictionary size 16384 for the 8th layer of the Pythia 160M and the 12th layer of Gemma 2 2B.

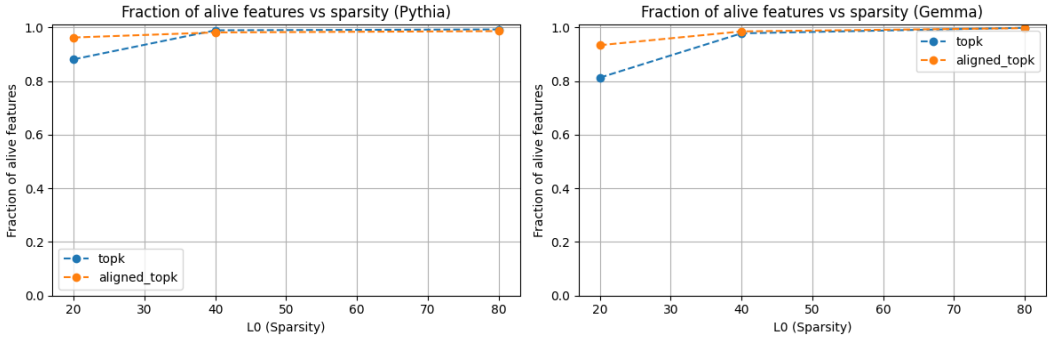

Figure 11: The proposed training method applied to TopK sparse autoencoders reduces the number of dead neurons for low sparsity. However, for larger sparsity, in both cases, there is almost none dead neurons. The results for the dictionary size 16384 for the 8th layer of the Pythia 160M and 12th layer of Gemma 2 2B.

by a different issue—bimodality and low-quality/dead features. It would be instructive to compare these approaches and explore whether they overlap or achieve synergy when applied together.

References

[1] Jonathan Marcus Adly Templeton, Tom Conerly and Tom Henighan. Update on dictionary learning improvements. *Transformer Circuits Thread*, 2024. URL `https://transformer-circuits.pub/2024/march-update/index.html#dl-update`.

[2] Lee Sharkey Benjamin Wright. Addressing feature suppression in saes. *AI Alignment Forum*, 2024. URL `https://www.alignmentforum.org/posts/3JuSjTZyMzaSeTxKk/addressing-feature-suppression-in-saes`.

[3] Stella Biderman, Hailey Schoelkopf, Quentin Gregory Anthony, Herbie Bradley, Kyle O'Brien, Eric Hallahan, Mohammad Aflah Khan, Shivanshu Purohit, USVSN Sai Prashanth, Edward Raff, et al. Pythia: A suite for analyzing large language models across training and scaling. In *International Conference on Machine Learning*, pages 2397–2430. PMLR, 2023.

[4] Steven Bills, Nick Cammarata, Dan Mossing, Henk Tillman, Leo Gao, Gabriel Goh, Ilya Sutskever, Jan Leike, Jeff Wu, and William Saunders. Language models can explain neurons in language models, 2023. URL https://openaipublic.blob.core.windows.net/neuron-explainer/paper/index.html.

[5] Joseph Bloom, Curt Tigges, Anthony Duong, and David Chanin. Saelens. https://github.com/jbloomAus/SAELens, 2024.

[6] Trenton Bricken, Adly Templeton, Joshua Batson, Brian Chen, Adam Jermyn, Tom Conerly, Nick Turner, Cem Anil, Carson Denison, Amanda Askell, Robert Lasenby, Yifan Wu, Shauna Kravec, Nicholas Schiefer, Tim Maxwell, Nicholas Joseph, Zac Hatfield-Dodds, Alex Tamkin, Karina Nguyen, Brayden McLean, Josiah E Burke, Tristan Hume, Shan Carter, Tom Henighan, and Christopher Olah. Towards monosemanticity: Decomposing language models with dictionary learning. *Transformer Circuits Thread*, 2023. URL https://transformer-circuits.pub/2023/monosemantic-features/index.html.

[7] Bart Bussmann, Patrick Leask, and Neel Nanda. Batchtopk sparse autoencoders. In *NeurIPS 2024 Workshop on Scientific Methods for Understanding Deep Learning*, 2024. URL https://openreview.net/forum?id=d4dpOCqybL.

[8] Tom Conerly, Adly Templeton, Trenton Bricken, Jonathan Marcus, and Tom Henighan. Update on dictionary learning improvements. *Transformer Circuits Thread*, 2024. URL https://transformer-circuits.pub/2024/april-update/index.html#training-saes.

[9] Hoagy Cunningham. Autointerpretation finds sparse coding beats alternatives. *AI Alignment Forum*, 2023. URL https://www.alignmentforum.org/posts/ursraZGcpfMjCXtnn/autointerpretation-finds-sparse-coding-beats-alternatives.

[10] Hoagy Cunningham and Logan Riggs. [replication] conjecture's sparse coding in small transformers. *Less Wrong*, 2023. URL https://www.lesswrong.com/posts/vBcsAw4rvLsri3JAj/replication-conjecture-s-sparse-coding-in-small-transformers.

[11] Maria De-Arteaga, Alexey Romanov, Hanna Wallach, Jennifer Chayes, Christian Borgs, Alexandra Chouldechova, Sahin Geyik, Krishnaram Kenthapadi, and Adam Tauman Kalai. Bias in bios: A case study of semantic representation bias in a high-stakes setting. In *Proceedings of the Conference on Fairness, Accountability, and Transparency*, FAT* '19, page 120–128, New York, NY, USA, 2019. Association for Computing Machinery. ISBN 9781450361255. doi: 10.1145/3287560.3287572. URL https://doi.org/10.1145/3287560.3287572.

[12] Nelson Elhage, Tristan Hume, Catherine Olsson, Nicholas Schiefer, Tom Henighan, Shauna Kravec, Zac Hatfield-Dodds, Robert Lasenby, Dawn Drain, Carol Chen, Roger Grosse, Sam McCandlish, Jared Kaplan, Dario Amodei, Martin Wattenberg, and Christopher Olah. Toy models of superposition. *Transformer Circuits Thread*, 2022. URL https://transformer-circuits.pub/2022/toy_model/index.html.

[13] Kunihiko Fukushima. Neocognitron: A hierarchical neural network capable of visual pattern recognition. *Neural Networks*, 1(2):119–130, 1988. ISSN 0893-6080. doi: https://doi.org/10.1016/0893-6080(88)90014-7. URL https://www.sciencedirect.com/science/article/pii/0893608088900147.

[14] Leo Gao, Stella Biderman, Sid Black, Laurence Golding, Travis Hoppe, Charles Foster, Jason Phang, Horace He, Anish Thite, Noa Nabeshima, Shawn Presser, and Connor Leahy. The Pile: An 800gb dataset of diverse text for language modeling. *arXiv preprint arXiv:2101.00027*, 2020.

[15] Leo Gao, Tom Dupre la Tour, Henk Tillman, Gabriel Goh, Rajan Troll, Alec Radford, Ilya Sutskever, Jan Leike, and Jeffrey Wu. Scaling and evaluating sparse autoencoders. In *The Thirteenth International Conference on Learning Representations*, 2025. URL https://openreview.net/forum?id=tcsZt9ZNKD.

[16] Robert Huben. [research update] sparse autoencoder features are bimodal. *From AI to ZI*, 2023. URL https://aizi.substack.com/p/research-update-sparse-autoencoder.

[17] Robert Huben, Hoagy Cunningham, Logan Riggs Smith, Aidan Ewart, and Lee Sharkey. Sparse autoencoders find highly interpretable features in language models. In *The Twelfth International Conference on Learning Representations*, 2023.

[18] Adam Jermyn and Adly Templeton. Ghost grads: An improvement on resampling. *Transformer Circuits Thread*, 2024. URL https://transformer-circuits.pub/2024/jan-update/index.html#dict-learning-resampling.

[19] Adam Jermyn, Adly Templeton, Joshua Batson, and Trenton Bricken. Tanh penalty in dictionary learning. *Transformer Circuits Thread*, 2024. URL https://transformer-circuits.pub/2024/feb-update/index.html#dict-learning-tanh.

[20] Adam Karvonen, Can Rager, Samuel Marks, and Neel Nanda. Evaluating sparse autoencoders on targeted concept erasure tasks, 2024. URL https://arxiv.org/abs/2411.18895.

[21] Adam Karvonen, Benjamin Wright, Can Rager, Rico Angell, Jannik Brinkmann, Logan Riggs Smith, Claudio Mayrink Verdun, David Bau, and Samuel Marks. Measuring progress in dictionary learning for language model interpretability with board game models. In *ICML 2024 Workshop on Mechanistic Interpretability*, 2024. URL https://openreview.net/forum?id=qzsDKwGJyB.

[22] Adam Karvonen, Can Rager, Johnny Lin, Curt Tigges, Joseph Bloom, David Chanin, Yeu-Tong Lau, Eoin Farrell, Callum McDougall, Kola Ayonrinde, Demian Till, Matthew Wearden, Arthur Conmy, Samuel Marks, and Neel Nanda. Saebench: A comprehensive benchmark for sparse autoencoders in language model interpretability, 2025. URL https://arxiv.org/abs/2503.09532.

[23] Y. Lecun, L. Bottou, Y. Bengio, and P. Haffner. Gradient-based learning applied to document recognition. *Proceedings of the IEEE*, 86(11):2278–2324, 1998. doi: 10.1109/5.726791.

[24] Jannik Brinkmann Logan Riggs Smith. Improving sae's by sqrt()-ing l1 & removing lowest activating features. *AI Alignment Forum*, 2024. URL https://www.alignmentforum.org/posts/YiGs8qJ8aNBgwt2YN/improving-sae-s-by-sqrt-ing-l1-and-removing-lowest.

[25] Luke Marks, Alasdair Paren, David Krueger, and Fazl Barez. Enhancing neural network interpretability with feature-aligned sparse autoencoders, 2024. URL https://arxiv.org/abs/2411.01220.

[26] Samuel Marks, Can Rager, Eric J Michaud, Yonatan Belinkov, David Bau, and Aaron Mueller. Sparse feature circuits: Discovering and editing interpretable causal graphs in language models. In *The Thirteenth International Conference on Learning Representations*, 2025. URL https://openreview.net/forum?id=I4e82CIDxv.

[27] Gonçalo Santos Paulo, Alex Troy Mallen, Caden Juang, and Nora Belrose. Automatically interpreting millions of features in large language models. In *Forty-second International Conference on Machine Learning*, 2025. URL https://openreview.net/forum?id=EemtbhJOXc.

[28] Senthooran Rajamanoharan, Arthur Conmy, Lewis Smith, Tom Lieberum, Vikrant Varma, János Kramár, Rohin Shah, and Neel Nanda. Improving sparse decomposition of language model activations with gated sparse autoencoders. In A. Globerson, L. Mackey, D. Belgrave, A. Fan, U. Paquet, J. Tomczak, and C. Zhang, editors, *Advances in Neural Information Processing Systems*, volume 37, pages 775–818. Curran Associates, Inc., 2024. URL https://proceedings.neurips.cc/paper_files/paper/2024/file/01772a8b0420baec00c4d59fe2fbace6-Paper-Conference.pdf.

[29] Senthooran Rajamanoharan, Tom Lieberum, Nicolas Sonnerat, Arthur Conmy, Vikrant Varma, Janos Kramar, and Neel Nanda. Jumping ahead: Improving reconstruction fidelity with jumpreLU sparse autoencoders, 2025. URL https://openreview.net/forum?id=mMPaQzgzAN.

[30] Logan Riggs. (tentatively) found 600+ monosemantic features in a small lm using sparse autoencoders. *AI Alignment Forum*, 2023. URL https://www.alignmentforum.org/posts/wqRqb7h6ZC48iDgfK/tentatively-found-600-monosemantic-features-in-a-small-lm.

[31] Alex Rogozhnikov. Einops: Clear and reliable tensor manipulations with einstein-like notation. In *International Conference on Learning Representations*, 2022. URL https://openreview.net/forum?id=oapKSVM2bcj.

[32] Adam Karvonen Samuel Marks and Aaron Mueller. dictionary_learning, 2024. URL https://github.com/saprmarks/dictionary_learning.

[33] Lee Sharkey, Dan Braun, and Beren Millidge. Taking features out of superposition with sparse autoencoders. *Alignment Forum*, 2023. URL https://www.alignmentforum.org/posts/z6QQJbtpkEAX3Aojj/interim-research-report-taking-features-out-of-superposition.

[34] Gemma Team, Morgane Riviere, Shreya Pathak, Pier Giuseppe Sessa, Cassidy Hardin, Surya Bhupatiraju, Léonard Hussenot, Thomas Mesnard, Bobak Shahriari, Alexandre Ramé, Johan Ferret, Peter Liu, Pouya Tafti, Abe Friesen, Michelle Casbon, Sabela Ramos, Ravin Kumar, Charline Le Lan, Sammy Jerome, Anton Tsitsulin, Nino Vieillard, Piotr Stanczyk, Sertan Girgin, Nikola Momchev, Matt Hoffman, Shantanu Thakoor, Jean-Bastien Grill, Behnam Neyshabur, Olivier Bachem, Alanna Walton, Aliaksei Severyn, Alicia Parrish, Aliya Ahmad, Allen Hutchison, Alvin Abdagic, Amanda Carl, Amy Shen, Andy Brock, Andy Coenen, Anthony Laforge, Antonia Paterson, Ben Bastian, Bilal Piot, Bo Wu, Brandon Royal, Charlie Chen, Chintu Kumar, Chris Perry, Chris Welty, Christopher A. Choquette-Choo, Danila Sinopalnikov, David Weinberger, Dimple Vijaykumar, Dominika Rogozińska, Dustin Herbison, Elisa Bandy, Emma Wang, Eric Noland, Erica Moreira, Evan Senter, Evgenii Eltyshev, Francesco Visin, Gabriel Rasskin, Gary Wei, Glenn Cameron, Gus Martins, Hadi Hashemi, Hanna Klimczak-Plucińska, Harleen Batra, Harsh Dhand, Ivan Nardini, Jacinda Mein, Jack Zhou, James Svensson, Jeff Stanway, Jetha Chan, Jin Peng Zhou, Joana Carrasqueira, Joana Iljazi, Jocelyn Becker, Joe Fernandez, Joost van Amersfoort, Josh Gordon, Josh Lipschultz, Josh Newlan, Ju yeong Ji, Kareem Mohamed, Kartikeya Badola, Kat Black, Katie Millican, Keelin McDonell, Kelvin Nguyen, Kiranbir Sodhia, Kish Greene, Lars Lowe Sjoesund, Lauren Usui, Laurent Sifre, Lena Heuermann, Leticia Lago, Lilly McNealus, Livio Baldini Soares, Logan Kilpatrick, Lucas Dixon, Luciano Martins, Machel Reid, Manvinder Singh, Mark Iverson, Martin Görner, Mat Velloso, Mateo Wirth, Matt Davidow, Matt Miller, Matthew Rahtz, Matthew Watson, Meg Risdal, Mehran Kazemi, Michael Moynihan, Ming Zhang, Minsuk Kahng, Minwoo Park, Mofi Rahman, Mohit Khatwani, Natalie Dao, Nenshad Bardoliwalla, Nesh Devanathan, Neta Dumai, Nilay Chauhan, Oscar Wahltinez, Pankil Botarda, Parker Barnes, Paul Barham, Paul Michel, Pengchong Jin, Petko Georgiev, Phil Culliton, Pradeep Kuppala, Ramona Comanescu, Ramona Merhej, Reena Jana, Reza Ardeshir Rokni, Rishabh Agarwal, Ryan Mullins, Samaneh Saadat, Sara Mc Carthy, Sarah Cogan, Sarah Perrin, Sébastien M. R. Arnold, Sebastian Krause, Shengyang Dai, Shruti Garg, Shruti Sheth, Sue Ronstrom, Susan Chan, Timothy Jordan, Ting Yu, Tom Eccles, Tom Hennigan, Tomas Kocisky, Tulsee Doshi, Vihan Jain, Vikas Yadav, Vilobh Meshram, Vishal Dharmadhikari, Warren Barkley, Wei Wei, Wenming Ye, Woohyun Han, Woosuk Kwon, Xiang Xu, Zhe Shen, Zhitao Gong, Zichuan Wei, Victor Cotruta, Phoebe Kirk, Anand Rao, Minh Giang, Ludovic Peran, Tris Warkentin, Eli Collins, Joelle Barral, Zoubin Ghahramani, Raia Hadsell, D. Sculley, Jeanine Banks, Anca Dragan, Slav Petrov, Oriol Vinyals, Jeff Dean, Demis Hassabis, Koray Kavukcuoglu, Clement Farabet, Elena Buchatskaya, Sebastian Borgeaud, Noah Fiedel, Armand Joulin, Kathleen Kenealy, Robert Dadashi, and Alek Andreev. Gemma 2: Improving open language models at a practical size, 2024. URL https://arxiv.org/abs/2408.00118.

[35] Zhengxuan Wu, Aryaman Arora, Atticus Geiger, Zheng Wang, Jing Huang, Dan Jurafsky, Christopher D Manning, and Christopher Potts. Axbench: Steering LLMs? even simple baselines outperform sparse autoencoders. In *Forty-second International Conference on Machine Learning*, 2025. URL https://openreview.net/forum?id=K2CckZjNy0.

A Technical details

In this appendix, we provide all the technical details necessary to replicate the conducted experiments. For loading pretrained SAEs, we used the sae-lens framework [5]. In histograms 1, we utilized the following SAEs:

- For Pythia: Model 70M, residual stream at layer 3. Sae-lens release: *pythia-70m-deduped-res-sm*, id: *blocks.3.hook_resid_post*.
- For LLaMA: Model 3 8B IT, residual stream at layer 25. Sae-lens release: *llama-3-8b-it-res-jh*, id: *blocks.25.hook_resid _post*.
- For Gemma: Model 2 2B, residual stream at layer 12. Sae-lens release: *sae_bench_gemma-2-2b_topk_width-2pow12_date-1109*, id: *blocks.12.hook_resid_post__trainer_0*.

For scatter plots 2 and 3 we used the ReLU autoencoders from [30]: *https://huggingface.co/Elriggs/autoencoder_layer_2_pythia70M_5_epochs*.

For autointerpretability we used the code *https://github.com/HoagyC/sparse_coding* which we modified to use the open source model Gemma 3 27B IT as a judge instead of the close source GPT.

For the remaining experiments, we used the same settings as in SAEBench, specifically layer 8 of Pythia 160M and layer 12 of Gemma 2 2B.

B Formulas for the reconstruction metrics

Explained variance is defined as

$$1 - \frac{\frac{1}{K}\sum_{k=1}^{K} ||\mathbf{x}_k - \hat{\mathbf{x}_k}||^2}{\frac{1}{K}\sum_{k=1}^{K} ||\mathbf{x}_k - \boldsymbol{\mu}||^2},$$

where $\boldsymbol{\mu}$ is the mean activation vector:

$$\boldsymbol{\mu} = \sum_{k=1}^{K} \mathbf{x}_k.$$

Cross entropy loss recovered is equal to

$$\frac{H^* - H_0}{H_{orig} - H_0},$$

where H_{orig} refers to the cross-entropy loss calculated for the model's next-token prediction task. H^* represents the cross-entropy loss obtained by replacing the model's activation $\mathbf{x}$ with its SAE-reconstructed version $\hat{x}$ during the forward pass. Additionally, H_0 denotes the cross-entrop loss that results from zeroing out the activation $\mathbf{x}$.

C Code implementation

For training our autoencoders, we utilized the code [32] and implemented the key transform 2 using the Python function described below. For the calculating the inner products per feature, we employed the einops [31] library, which provides flexible Einstein notation operations on tensors.

```
def get_the_encoder_matrix(dict_size: int, encoder_weights_orthogonal_part:
↪  Float[Tensor, "activation_dim-1 dict_size"], decoder_weights:
↪  Float[Tensor, "dict_size activation_dim"]) -> Float[Tensor,
↪  "activation_dim dict_size"]:
    zeros = torch.zeros(1, dict_size).to(encoder_weights_orthogonal_part)
    appended = torch.concat([encoder_weights_orthogonal_part, zeros])
    inner_products = einops.einsum(decoder_weights, appended, "dict_size
    ↪  activation_dim, activation_dim dict_size -> dict_size")
    decoder_norms_squared = decoder_weights.pow(2).sum(dim=1)
    reparametrized = appended + decoder_weights.T * (1 - inner_products) /
    ↪  decoder_norms_squared
    return reparametrized
```

D Additional experimental results

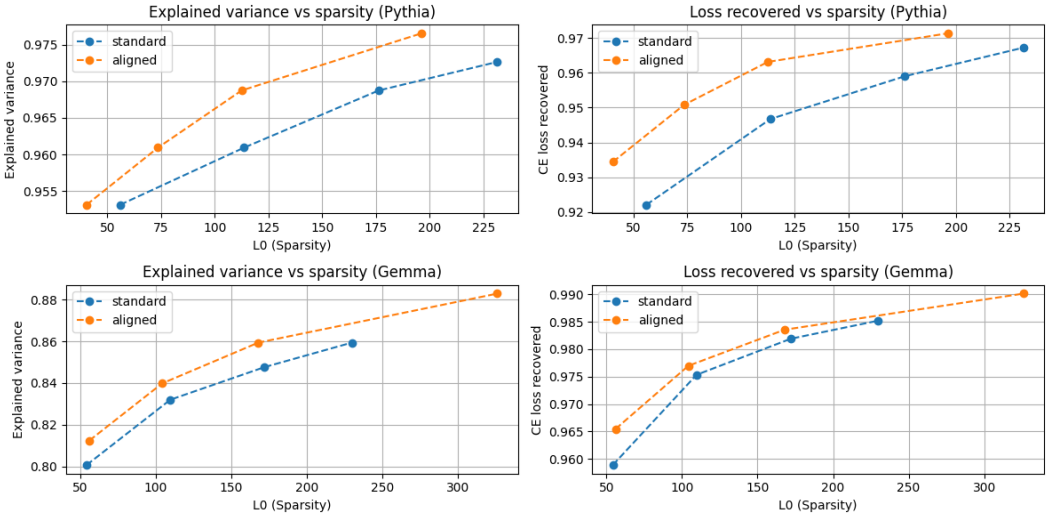

Figure 12: Reconstruction metrics for Pythia 160M layer 8 and Gemma 2 2B layer 12 and the dictionary size of 16384 features.

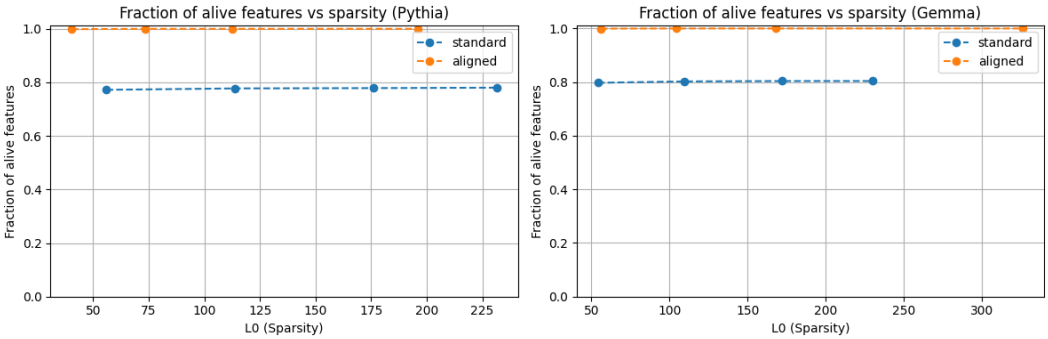

Figure 13: Fraction of alive neurons for Pythia 160M layer 8 and Gemma 2 2B layer 12 and the dictionary size of 16384 features.

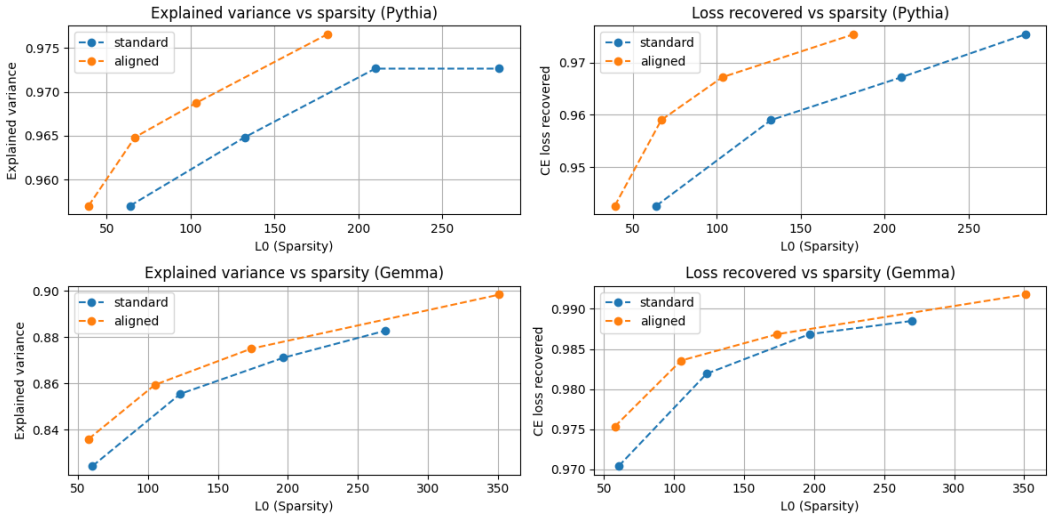

Figure 14: Reconstruction metrics for Pythia 160M layer 8 and Gemma 2 2B layer 12 and the dictionary size of 65K features.

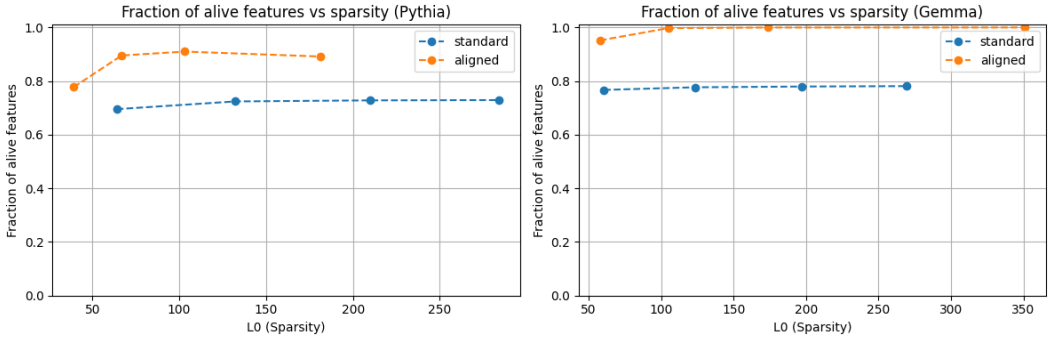

Figure 15: Fraction of alive neurons for Pythia 160M layer 8 and Gemma 2 2B layer 12 and the dictionary size of 65K features.

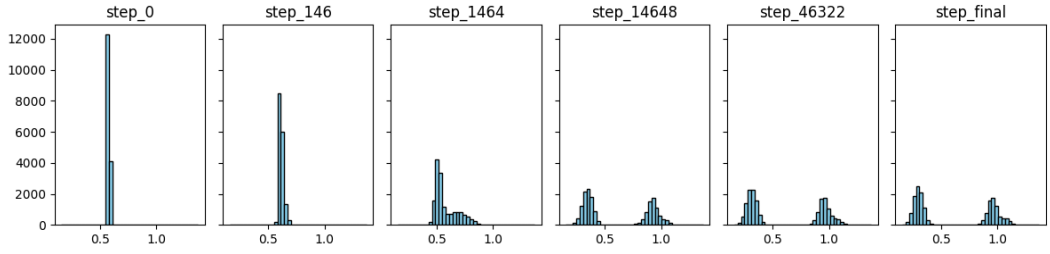

Figure 16: Creation of the bimodality during training of a TopK SAE trained on the layer 12 of Gemma 2 2B. We used checkpoints provided in SAEBench[22]. We hypotesize that this is caused by two competing forces: useful features are pushed to the cluster with the alignment close to 1. On the other hand, useless features are pushed to the left, where they rarely activate. The second effect is caused by the sparsity goal.